

The Massive Progenitor of the Type II-Linear Supernova 2009kr¹

Nancy Elias-Rosa², Schuyler D. Van Dyk², Weidong Li³, Adam A. Miller³, Jeffrey M. Silverman³, Mohan Ganeshalingam³, Andrew F. Boden⁴, Mansi M. Kasliwal⁴, József Vinkó^{5,6}, Jean-Charles Cuillandre⁷, Alexei V. Filippenko³, Thea N. Steele³, Joshua S. Bloom³, Christopher V. Griffith³, Io K. W. Kleiser³, and Ryan J. Foley^{8,9}

ABSTRACT

We present early-time photometric and spectroscopic observations of supernova (SN) 2009kr in NGC 1832. We find that its properties to date support its classification as Type II-linear (SN II-L), a relatively rare subclass of core-collapse supernovae (SNe). We have also identified a candidate for the SN progenitor star through comparison of pre-explosion, archival images taken with WFPC2 onboard the *Hubble Space Telescope* with SN images obtained using adaptive optics (AO) plus NIRC2 on the 10-m Keck-II telescope. Although the host galaxy's substantial distance (~ 26 Mpc) results in large uncertainties in the relative astrometry, we find that if this candidate is indeed the progenitor, it is a highly luminous ($M_V^0 = -7.8$ mag) yellow supergiant with initial mass $\sim 18\text{--}24 M_\odot$. This would be the first time that a SN II-L progenitor has been directly identified. Its mass may be a bridge between the upper initial mass limit for the more common Type II-plateau SNe (SNe II-P) and the inferred initial mass estimate for one Type II-narrow SN (SN II_n).

Subject headings: galaxies: individual (NGC 1832) — stars: evolution — supernovae: general — supernovae: individual (SN 2009kr)

²Spitzer Science Center, California Institute of Technology, 1200 E. California Blvd., Pasadena, CA 91125; email nelias@ipac.caltech.edu.

³Department of Astronomy, University of California, Berkeley, CA 94720-3411.

⁴Division of Physics, Math, and Astronomy, California Institute of Technology, Pasadena, CA 91125.

⁵Department of Optics & Quantum Electronics, University of Szeged, Dóm tér 9, Szeged H-6720, Hungary.

⁶Department of Astronomy, University of Texas, Austin, TX 78712.

⁷Canada-France-Hawaii Telescope Corporation, 65-1238 Mamalahoa Hwy, Kamuela, HI 96743.

⁸Harvard-Smithsonian Center for Astrophysics, 60 Garden Street, Cambridge, MA 02138.

⁹Clay Fellow.

1. Introduction

It is not yet exactly clear how to map massive stars of a given mass range to a core-collapse supernova (CC SN) subtype. We now know with a growing degree of confidence that solitary stars in the range of $\sim 8\text{--}16 M_{\odot}$ inevitably explode as Type II-plateau supernovae (SNe II-P; e.g., Smartt et al. 2009), with much of their hydrogen envelope still intact (see Filippenko 1997 for a discussion of SN classification). We also have evidence that the Type II-narrow (IIn) SN 2005gl had a luminous ($M_V = -10.3$ mag), very massive (possibly with initial mass $M_{\text{ini}} > 50 M_{\odot}$) progenitor star that exploded while in the luminous blue variable phase (Gal-Yam & Leonard 2009). This progenitor, the only example so far identified for a SN IIn, likely had a far smaller fraction of its outer H layer remaining than do SNe II-P. Various indirect clues may indicate that at least some of the Type Ib/c SNe are connected to the Wolf-Rayet phase, which is expected to occur for stars with $M_{\text{ini}} > 25\text{--}30 M_{\odot}$ (e.g., Crowther 2007). That leaves the Type II-linear (II-L) SNe with no directly known progenitor star, as well as the range $M_{\text{ini}} = 18\text{--}30 M_{\odot}$ (exactly the range that Smartt et al. 2009 dubbed “the red supergiant problem”) without a well-established endpoint. From the rates derived with the Lick Observatory Supernova Search (LOSS) for a sample of well-studied SNe (Li et al. 2010, in prep.), we know that the majority of massive stars end their lives as SNe II-P, while the incidences of SNe II-L and SNe IIn are comparatively rare ($\sim 7\%$ and $\sim 6\%$ of all CC SNe, respectively).

Here we examine the case of SN 2009kr in NGC 1832. SN 2009kr was discovered by Nakano & Itagaki (2009) on 2009 Nov. 6.73 (UT dates are used throughout) and was spectroscopically classified as a SN IIn (Tendulkar et al. 2009), and then as a “young type-II” SN (Steele et al. 2009). Li et al. (2009) first identified a possible progenitor star in archival *HST* images from 2004, using as reference a combined 160-s r' image from CFHT+MegaCam¹⁰ on Nov. 21.49. Here we show that both early-time photometric and

¹Based in part on observations made with the NASA/ESA *Hubble Space Telescope (HST)*, obtained from the Data Archive at the Space Telescope Science Institute, which is operated by the Association of Universities for Research in Astronomy (AURA), Inc., under NASA contract NAS 05-26555; the 6.5-m Magellan Clay Telescope located at Las Campanas Observatory, Chile; various telescopes at Lick Observatory; the 1.3-m PAIRITEL on Mt. Hopkins; the SMARTS Consortium 1.3-m telescope located at Cerro Tololo Inter-American Observatory (CTIO), Chile; the 3.6-m Canada-France-Hawaii Telescope (CFHT), which is operated by the National Research Council of Canada, the Institut National des Sciences de l’Univers of the Centre National de la Recherche Scientifique of France, and the University of Hawaii; and the W. M. Keck Observatory, which is operated as a scientific partnership among the California Institute of Technology, the University of California, and NASA, with generous financial support from the W. M. Keck Foundation.

¹⁰A joint project of CFHT and CEA/DAPNIA.

spectroscopic observations strongly suggest that this object is a SN II-L, and we increase our confidence in the progenitor identification via further comparison of the *HST* images with Keck-II/NIRC2 adaptive-optics (AO) data.

2. The Early-Time Nature of SN 2009kr

2.1. Photometry

Optical *BVRI* images of SN 2009kr were obtained with the Lick Observatory 0.76-m Katzman Automatic Imaging Telescope (KAIT; Filippenko et al. 2001) and the 1.0-m Nickel telescope, and SMARTS+ANDICAM at CTIO. They were all initially reduced using standard procedures (see, e.g., Poznanski et al. 2009). Because of our follow-up campaign on SN 2004gq (Modjaz 2007), also in NGC 1832, we had a well-calibrated photometric sequence in the host-galaxy field and template images in all passbands for image subtraction. We used an image-reduction pipeline (Ganeshalingam et al. 2010) to reduce all data and calibrate the photometry to the standard Johnson *BV* and Cousins *RI* system.

Near-infrared (NIR) observations were obtained with the 1.3-m Peters Automated Infrared Imaging Telescope (PAIRITEL; Bloom et al. 2006) and reduced using standard procedures. We used archival 2MASS images of NGC 1832 as templates to subtract from the SN images using HOTPANTS¹¹ and calibrated the *JHK_s* photometry against 2MASS stars in the field.

The *BVRIJHK_s* light curves are shown in Figure 1(a), relative to *B*-band maximum (15.95 ± 0.02 mag on Nov. 13 ± 1 , or JD 2,455,149 ± 1). For comparison, we also show the light curves of the SNe II-L 1979C (Balinskaia et al. 1980; de Vaucouleurs et al. 1981; Barbon et al. 1982b), 1980K (Buta 1982; Dwek et al. 1983), 1990K (Cappellaro et al. 1995), and 2001cy (unpublished KAIT data); the SNe II-P 1999em (Hamuy et al. 2001; Leonard et al. 2002) and 1992H (Clocchiatti et al. 1996); and, the possible SN II-L 2000dc (Poznanski et al. 2009). SN 2009kr does not follow the SN II-P plateau; instead, it more closely resembles the SN II-L linear decline (see Barbon et al. 1979). A steeper decline is present in *VRI* after ~ 65 days in the SN 2009kr light curves; however, this decline was also observed for SN 1980K in *V*. From our adopted distance and total extinction (see §2.2), SN 2009kr reached $M(B_{\max}) = -16.48 \pm 0.30$ mag, typical of SNe II-L (Young & Branch 1989). We thus conclude that SN 2009kr displays the photometric behavior of a SN II-L.

¹¹<http://www.astro.washington.edu/users/becker/hotpants.html>.

2.2. Spectroscopy

Low-resolution spectra of SN 2009kr were obtained on 2009 Nov. 10 and 25, Dec. 9 and 18, and 2010 Jan. 20 with the Lick 3-m Shane telescope+Kast spectrograph (Miller & Stone 1993); on Jan. 8 with the Clay telescope+MagE (Marshall et al. 2008); on Feb. 15 with the 10-m Keck-II telescope+DEIMOS; and on Mar. 9 with the 10-m Keck-I telescope+LRIS. The spectra were reduced and calibrated using standard procedures (e.g., Matheson et al. 2000). The observing conditions were not photometric, resulting in uncertain absolute-flux calibrations. We observed with the slit placed at the parallactic angle (Filippenko 1982).

We show the rest-frame spectral sequence in Figure 1(b); for comparison, we also display spectra of the SN II-L 1980K (Barbon et al. 1982a); the SNe II-P 1999em (Leonard et al. 2002), 1992H (Clocchiatti et al. 1996) and 2004et (Sahu et al. 2006); and the SN II 2001cy at similar epochs. Poznanski et al. (2009) rejected SN 2001cy from their SN II-P sample, implying that it likely may be a SN II-L. Indeed, the SN 2001cy light curve is very similar (but of inferior quality and coverage) to that of SN 2000dc shown in Figure 1(a). The following corrections for $E(B - V)_{\text{tot}}$ have been made: SN 1999em (0.10 mag, Leonard et al. 2002), SN 1992H (0.09 mag, Clocchiatti et al. 1996), SN 2004et (0.41 mag, Maguire et al. 2010), SN 1980K (0.40 mag, Barbon et al. 1982a), and SN 2009kr (0.08 mag; see below). SN 2001cy has been corrected only for Galactic reddening, $E(B - V)_{\text{Gal}} = 0.21$ mag (Schlegel et al. 1998).

The spectral sequence for SN 2009kr is typical of many SNe II: the earliest spectra exhibit a blue continuum, with relatively weak spectral features, followed by the onset of increased Balmer-line emission, together with the emergence of P-Cygni-like features. However, clearly SN 2009kr differs from the canonical SN 1999em or the peculiar SNe 1992H and 2004et; in particular, the SN 2009kr P-Cygni $H\alpha$ profile is dominated by the broad emission component. Several narrow emission lines appear superposed on the spectra, but these most likely originate from a neighboring H II region, seen $\sim 1\text{--}2''$ northeast of the SN in an $H\alpha$ image of the host galaxy (unpublished ESO archival data; the region’s ionizing cluster can also be seen in the *HST* images). The SN 2009kr spectra more closely resemble those of SN 1980K or SN 2001cy, which also exhibit relatively weak $H\alpha$ absorption. The optical photometric decline rates [$\gtrsim 1$ mag (100 day) $^{-1}$] of SNe 1980K, 2001cy, and 2009kr suggest that they are all SNe II-L (see § 2.1). Since spectroscopic features of SNe II appear to be correlated with their photometric behavior at early times (Schlegel 1996; Filippenko 1997), the similarities in the spectra of these three SNe are not unexpected.

We also obtained a high-resolution optical spectrum of SN 2009kr on 2009 Nov. 25.46 with CFHT+ESPaDOnS, with 4 exposures of 833 s each, from which we confirm that the narrow $H\alpha$ emission likely originates from the H II region. Moreover, we also used this spectrum

to estimate the reddening toward SN 2009kr via measurement of the Na I D equivalent width (EW) at the host-galaxy redshift ($z = 0.006$). We found $\text{EW}(\text{Na I D1 } \lambda 5890) = 0.044 \pm 0.003 \text{ \AA}$ and $\text{EW}(\text{Na I D2 } \lambda 5896) = 0.032 \pm 0.004 \text{ \AA}$. Using the relation between extinction and $\text{EW}(\text{Na I D})$ from Elias-Rosa et al. (2010, in prep.), and assuming the Cardelli et al. (1989) reddening law with updated wavelengths and a Galactic foreground $E(B - V) = 0.07 \text{ mag}$ (Schlegel et al. 1998), we derive $E(B - V)_{\text{tot}} = 0.08 \pm 0.01 \text{ mag}$ ($E[V - I]_{\text{tot}} = 0.11 \pm 0.01 \text{ mag}$), which we adopt for the SN. This relatively low extinction is consistent with both the SN color comparison (§ 2.1) and the overall blue continua seen in the early-time SN 2009kr spectra (Fig. 1[b]).

3. Identification of the Progenitor Candidate

Pairs of *HST* images of NGC 1832 were obtained with WFPC2 in bands F555W ($\sim V$; 460 s total) and F814W ($\sim I$; 700 s total) on 2008 Jan. 11 (program GO-10877, PI: W. Li), as SN 2004gq follow-up observations. The SN 2009kr site is located on the WF3 chip ($0'.1 \text{ pixel}^{-1}$). Cosmic-ray hits were rejected, and a 1600×1600 pixel mosaic of all four WFPC2 chips was constructed using the STSDAS package routines *crrej* and *wmosaic* within IRAF¹². Li et al. (2009) were able to isolate the SN location in the WFPC2 images to 0.43 pixel ($0'.043$) through comparison with a ground-based, post-explosion CFHT+MegaCam image.

We were then able to better confirm the identification of this candidate through K_p -band NIRC2 “wide” camera ($0'.04 \text{ pixel}^{-1}$, $40'' \times 40''$ field of view) images obtained on 2009 Nov. 28 with Keck-II+AO. Each of the 10-s frames was sky subtracted using the median of the dithered exposures, and then “shifted-and-added” using IRAF. They were also corrected for distortion¹³.

We achieved high-precision relative astrometry by geometrically transforming the pre-explosion images to match the post-explosion ones. We first “drizzled”¹⁴ the pre-explosion images for each band to the higher NIRC2+AO resolution. Using 5–7 point-like sources in common between the two datasets and the IRAF tasks *geomap* and *geotran*, we carried out a geometrical transformation between the two sets of images. The positions (and their

¹²IRAF (Image Reduction and Analysis Facility) is distributed by the National Optical Astronomy Observatories, which are operated by the AURA, Inc., under cooperative agreement with the National Science Foundation (NSF).

¹³http://www.2.keck.hawaii.edu/inst/nirc2/forReDoc/post_observing/dewarp/.

¹⁴<http://www.stsci.edu/hst/wfpc2/analysis/drizzle.html>.

uncertainties) of the SN and the progenitor candidate are derived by averaging the measurements from two centroiding methods, the task *daofind* within IRAF/DAOPHOT and *imexamine* within IRAF. The differences between the SN and the progenitor candidate positions, compared with the total estimated astrometric uncertainty, are given in Table 1. As an additional check, we transformed the NIRC2+AO image relative to only the WF3 chip image in F814W at its native resolution ($0''.1 \text{ pixel}^{-1}$) and performed the registration. In this case, the positional difference is 19 mas, within $\sim 1\sigma$ of the uncertainty in the astrometric solution. Note that no other source was located within a 5σ radius from the progenitor candidate position identified by Li et al. (2009); the H II region to the northeast is located at $> 25\sigma$ (see Fig. 2).

4. The Nature of the Progenitor

We also measured photometry of the *HST* images using HSTphot¹⁵ (Dolphin 2000). The output from this package automatically includes the transformation from F555W and F814W to *V* and *I*.

Adopting a distance modulus to NGC 1832 derived from the recession velocity corrected for Virgo infall ($32.09 \pm 0.30 \text{ mag}$; this uncertainty arises from a possible 250 km s^{-1} peculiar velocity¹⁶) and the assumed SN extinction, we find that the absolute magnitudes of the progenitor candidate are $M_V^0 = -7.80 \pm 0.33$ and $M_I^0 = -8.75 \pm 0.32$, entirely consistent with a highly luminous supergiant. The intrinsic color, $(V - I)_0 = 0.95 \pm 0.21 \text{ mag}$, is significantly more “yellow” than the colors of normal red supergiants (RSGs; e.g., Drilling & Landolt 2000).

We can directly determine the metallicity in the SN environment from the CFHT high-resolution spectrum, by measuring the $H\alpha$ and $[\text{N II}] \lambda 6584$ line intensities and applying the (Pettini & Pagel 2004) cubic-fit relation between the ratio of these two lines and the oxygen abundance; no correction is made for the low extinction. Doing so, we find that $12 + \log(\text{O}/\text{H}) = 8.67$. Given that the solar value is 8.69 ± 0.05 (Asplund et al. 2009), we consider it most likely that this environment has roughly solar metallicity.

The star’s color corresponds to an effective temperature $T_{\text{eff}} = 5300 \pm 500 \text{ K}$ and a *V* bolometric correction in the range -0.47 to -0.13 mag , for an assumed surface gravity $\log g =$

¹⁵HSTphot is a stellar photometry package designed for use with WFPC2 images. We used v1.1.7b, updated 2008 July 19.

¹⁶From NED, <http://nedwww.ipac.caltech.edu/>.

+0.5 (Kurucz Atlas 9 models, CD-ROMs 13, 18). This results in $L_{\text{bol}} = 10^{(5.12 \pm 0.15)} L_{\odot}$ (assuming $M_{\text{bol}}(\odot) = 4.74$ mag). In Figure 3 we show a Hertzsprung-Russell (HR) diagram including the progenitor candidate. In addition, we illustrate model evolutionary tracks (Hirschi et al. 2004) for stars with $M_{\text{ini}} = 15, 20,$ and $25 M_{\odot}$, with rotation ($v_{\text{ini}} = 300 \text{ km s}^{-1}$) and without rotation.

The location of the progenitor candidate in the HR diagram is clearly not consistent with the $15 M_{\odot}$ tracks, an initial mass which lies within the range for SN II-P progenitors (Smartt et al. 2009). Unfortunately, the mass bins for these tracks are large ($5 M_{\odot}$ increments). However, taking into account the uncertainty in the progenitor candidate’s luminosity, interpolating by eye between the tracks implies that $M_{\text{ini}} \approx 18\text{--}24 M_{\odot}$. We note that this is consistent with the upper limit of $< 20 M_{\odot}$ on the SN 1980K progenitor (Smartt et al. 2009, using more current theoretical tracks) and the lower limit of $\gtrsim 17\text{--}18 M_{\odot}$ on the SN II-L 1979C progenitor (Van Dyk et al. 1999).

That such a massive progenitor would be somewhat bluer than would be expected for the normal RSG progenitors of SNe II-P is also consistent with the star being in a post-RSG phase. Such an expectation follows from the theoretical models by Hirschi et al. (2004) for rotating stars at higher masses; the rotating models are more luminous and evolve to the RSG phase before the ignition of He burning, which results in higher mass-loss rates, the loss of most of the H envelope before the termination of He burning, and evolution toward the blue before the terminal points. From Figure 3 one can see that rotation makes little difference in the evolution of a $15 M_{\odot}$ star; both the rotating and nonrotating tracks terminate as a RSG. However, for a $20 M_{\odot}$ star, rotation has a profound evolutionary effect. Though we cannot tell from these models what occurs for stars in the $15\text{--}20 M_{\odot}$ range, it is reasonable to assume that rotation begins to affect those models nearing $20 M_{\odot}$. Thus, we might expect the progenitor candidate, based on our mass estimate above, to have evolved toward the blue before explosion.

Although more luminous and hotter than the SN 2009kr progenitor candidate, similar behavior has occurred for the post-RSG star IRC+10420, a mass-losing hypergiant that is transiting the so-called “yellow void” (Humphreys et al. 2002). Likely more analogous are the “anomalous” yellow supergiants in the Magellanic Clouds, which are in the mass range $15\text{--}20 M_{\odot}$ and show evidence for post-RSG evolution (Humphreys et al. 1991), albeit at subsolar metallicity.

Of course, there are caveats; as we found for the peculiar SN II-P 2008cn (Elias-Rosa et al. 2009), a yellow progenitor color could result from evolution in an interacting binary. Additionally, although the difference between the SN and progenitor candidate positions are practically within the total uncertainties, these are still large, and, given the host galaxy’s

distance (a single NIRC2 pixel corresponds to ~ 5 pc), it is possible that we have not identified the SN progenitor at all, but rather a compact star cluster.

If so, adopting the SN extinction, we can fit the V and I fluxes for the progenitor candidate with the Starburst99 code¹⁷ model spectral energy distributions and find an excellent fit with a 10 Myr track (Fig. 4). If the SN progenitor were a member of this cluster, this age estimate would still be consistent with the lifespan of a $\sim 20 M_{\odot}$ star. The 8 Myr model also provides a good fit. However, the lowest possible cluster luminosity that exceeds the luminosity of the most massive 8 Myr-old star is $M_V \approx -8.1$ mag, and for 10 Myr it is $M_V \approx -7.6$ mag (Cerviño & Luridiana 2004). Both of these are roughly consistent with the candidate’s luminosity. Furthermore, we would ordinarily expect compact star clusters to have $M_V < -8.6$ mag (Bastian et al. 2005; Crockett et al. 2008). Additional dust obscuration, beyond our assumed extinction, would imply that a putative cluster could be more luminous, but it would also be bluer and younger.

A similar study has been done contemporaneously by Fraser et al. (2010), identifying the same candidate progenitor. However, Fraser et al. (2010) suggest that the SN is a spectrally peculiar SN II-P, with only r -band photometry reported. Differences also exist in the metallicity estimate and theoretical models employed, leading to somewhat different estimates for M_{ini} ($15_{-4}^{+5} M_{\odot}$ by Fraser et al. 2010).

5. Conclusions

Based on ~ 3 months of follow-up observations from discovery, we conclude that SN 2009kr is a SN II-L, a relatively rare subclass of CC SNe. We identified an object in pre-explosion *HST* images which agrees astrometrically with the SN 2009kr position, using NIR SN images obtained with NIRC2+AO on Keck. From the SN distance and extinction we find that the object is consistent with a highly luminous supergiant star. Placing the inferred L_{bol} and T_{eff} of the progenitor candidate on an HR diagram, we infer $M_{\text{ini}} \approx 18\text{--}24 M_{\odot}$. Its yellow color implies that the star may have exploded in a post-RSG evolutionary state, which is predicted by our assumed theoretical stellar models. If this star is the SN 2009kr progenitor, this would be *the first-ever direct identification of a SN II-L progenitor*. The star’s mass estimate also may be a link between the upper mass range for SNe II-P (Smartt et al. 2009) and the estimated progenitor mass for SN II_n 2005gl (Gal-Yam & Leonard 2009).

Ultimately, the definitive indication that we have identified the SN 2009kr progenitor is

¹⁷<http://www.stsci.edu/science/starburst99/>, Vazquez & Leitherer (2005).

through very late-time imaging, such as with *HST* (Maund & Smartt 2009). However, as a SN II-L, akin to the long-lasting SN 1979C (Milisavljevic et al. 2009), we may have to wait at least a decade to image the SN site using the *James Webb Space Telescope*.

We thank C. Blake, S. B. Cenko, B. Cobb, E. Falco, M. Kandrashoff, J. Kong, M. Modjaz, D. Starr, and T. Yuan for their assistance. J.V. received support from Hungarian OTKA Grant K76816, NSF Grant AST-0707769, and Texas Advanced Research Project grant ARP-0094. A.V.F.’s group and KAIT are supported by NSF grant AST-0908886, the Sylvia & Jim Katzman Foundation, the TABASGO Foundation, and NASA through grants AR-11248 and GO-10877 from STScI. PAIRITEL is operated by SAO with support from the Harvard University Milton Fund, UC Berkeley, University of Virginia, and NASA/*Swift* grant NNX09AQ66G. J.S.B. and his group are partially funded by a DOE SciDAC grant.

Facilities: HST (WFPC2); Lick: KAIT, Nickel, Shane; CFHT: MegaCam; Keck-I: LRIS; Keck-II: NIRC2+AO, DEIMOS; CTIO: SMARTS; Magellan: MagE

REFERENCES

- Asplund, M., Grevesse, N., Sauval, A. J. & Scott, P. 2009, *A&A Rev.*, 47, 481
- Balinskaia, I. S., Bychkov, K. V., & Neizvestnyi, S. I. 1980, *A&A*, 85, L19
- Barbon, R., Ciatti, F., & Rosino, L. 1979, *A&A*, 72, 287
- Barbon, R., Ciatti, F. & Rosino, L. 1982a, *A&A*, 116, 35
- Barbon, R., Ciatti, F., Rosino, L., Ortolani, S., & Rafanelli, P. 1982b, *A&A*, 116, 43
- Bastian, N., Gieles, M., Efremov, Y. N., & Lamers, H. J. G. L. M. 2005, *A&A*, 443, 79
- Bloom, J. S., et al. 2006, in *Astronomical Data Analysis Software and Systems XV*, ed. C. Gabriel, et al. (San Francisco: ASP, vol. 331), 751
- Buta, R. J. 1982, *PASP*, 94, 578
- Cappellaro, E., Danziger, I. J., Della Valle, M., Gouiffes, C., & Turatto, M. 1995, *A&A*, 293, 723
- Cardelli, J. A., Clayton, G. C., & Mathis, J. S. 1989, *ApJ*, 345, 245
- Cerviño, M., & Luridiana, V. 2004, *A&A*, 413, 145

- Clocchiatti, A., et al. 1996, *AJ*, 111, 1286
- Crockett, R. M., et al. 2008, *ApJ*, 672, L99
- Crowther, P. A. 2007, *ARA&A*, 45, 177
- de Vaucouleurs, G., de Vaucouleurs, A., Buta, R., Ables, H. D., & Hewitt, A. V. 1981, *PASP*, 93, 36
- Dolphin, A. E. 2000, *PASP*, 112, 1383
- Drilling, J. S. & Landolt, A. U. 2000, in *Allen’s Astrophysical Quantities*, ed. A. N. Cox (New York: Springer), 381
- Dwek, E., et al. 1983, *ApJ*, 274, 168
- Elias-Rosa, N., et al. 2009, *ApJ*, 706, 1174
- Filippenko, A. V. 1982, *PASP*, 94, 715
- Filippenko, A. V. 1997, *ARA&A*, 35, 309
- Filippenko, A. V., Li, W., Treffers, R. R., & Modjaz, M. 2001, in *Small Telescope Astronomy on Global Scales*, ed. W. P. Chen, C. Lemme, & B. Paczyński (San Francisco: ASP), 121
- Fraser, M., et al. 2010, *ApJL*, submitted (arXiv: 0912.2071)
- Gal-Yam, A., & Leonard, D. C. 2009, *Nature*, 458, 865
- Ganeshalingam, M., et al. 2010, *ApJS*, submitted
- Hamuy, M., et al. 2001, *ApJ*, 558, 615
- Hirschi, R., Meynet G., & Maeder A. 2004, *A&A*, 425, 649
- Humphreys, R. M., Kudritzki, R. P., & Groth, H. G. 1991, *A&A*, 245, 593
- Humphreys, R. M., Davidson, K., & Smith, N. 2002, *AJ*, 124, 1026
- Leonard, D. C., et al. 2002, *PASP*, 114, 35
- Li, W., et al. 2009, *CBET* 2042, 1
- Maguire, K., et al. 2010, *MNRAS*, in press., arXiv:0912.3111

- Marshall, J. L., et al. 2008, Society of Photo-Optical Instrumentation Engineers (SPIE) Conference Series, 7014
- Matheson T., Filippenko A. V., Ho L. C., Barth A. J., Leonard D. C., 2000, AJ, 120, 1499
- Maund, J. R., & Smartt, S. J. 2009, Science, 324, 486
- Milisavljevic, D., Fesen, R. A., Kirshner, R. P., & Challis, P. 2009, ApJ, 692, 839
- Miller, J. S., & Stone, R. P. S., 1993, Lick Observatory Technical Report No. 66, University of California, Santa Cruz
- Modjaz, M. 2007, Ph.D. Thesis, Harvard University
- Nakano, S., & Itagaki, K. 2009, CBET 2006, 1
- Pettini, M., & Pagel, B. E. J. 2004, MNRAS, 348, 59
- Poznanski, D., et al., 2009, ApJ, 694, 1067
- Sahu, D. K., Anupama, G. C., Srividya, S., & Muneer, S. 2006, MNRAS, 372, 1315
- Schlegel, E. M. 1996, AJ, 111, 1660
- Schlegel, D. J., Finkbeiner, D. P., & Davis, M. 1998, ApJ, 500, 525
- Smartt, S. J., et al. 2009, MNRAS, 395, 1409
- Steele, T. N., et al. 2009, CBET 2011, 1
- Tendulkar, S. P., et al. 2009, The Astronomer’s Telegram, 2291, 1
- Van Dyk, S. D., et al. 1999, PASP, 111, 313
- Vazquez, G. A., & Leitherer, C. 2005, ApJ, 621, 695
- Young, T. R., & Branch, D. 1989, ApJ, 342, L79

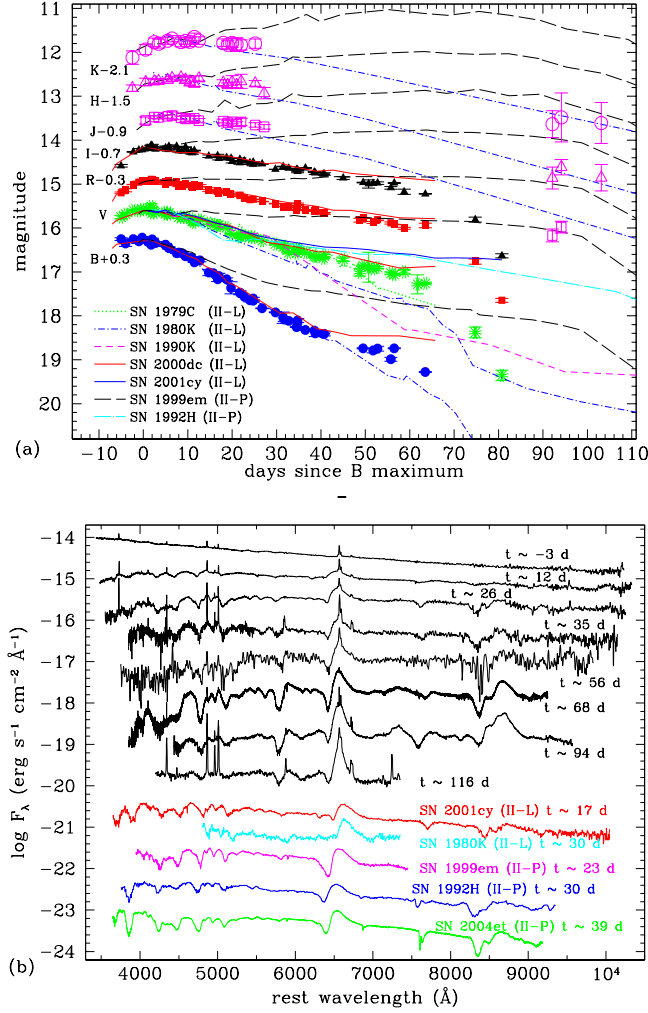


Fig. 1.— (a) SN 2009kr optical and NIR light curves, together with those of other SNe II-L and SNe II-P. The comparison light curves are adjusted in time and magnitude to match those of SN 2009kr. (b) SN 2009kr spectral sequence, along with comparison spectra of other SNe II-L and SNe II-P. All spectra have been corrected for their host-galaxy recession velocities and for reddening (see text). Ages are relative to B maximum light. The continuum of the $t \approx 116$ day spectrum of SN 2009kr appears to be significantly contaminated by light from the nearby star cluster.

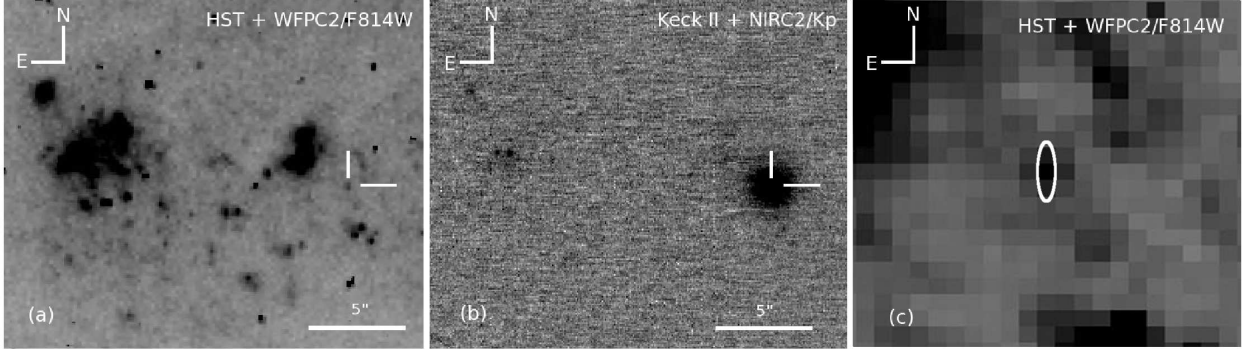


Fig. 2.— (a) Subsections of the pre-explosion *HST*+*WFPC2*/*F814W* images of NGC 1832, and (b) the post-explosion AO *K_p* image of SN 2009kr with Keck II+*NIRC2*. The approximate positions of the candidate progenitor and the SN are indicated by tick marks. (c) $5'' \times 5''$ detail of the *HST* image. The 3σ positional uncertainty ellipse is $0''.03 \times 0''.09$ in radius (see Table 1).

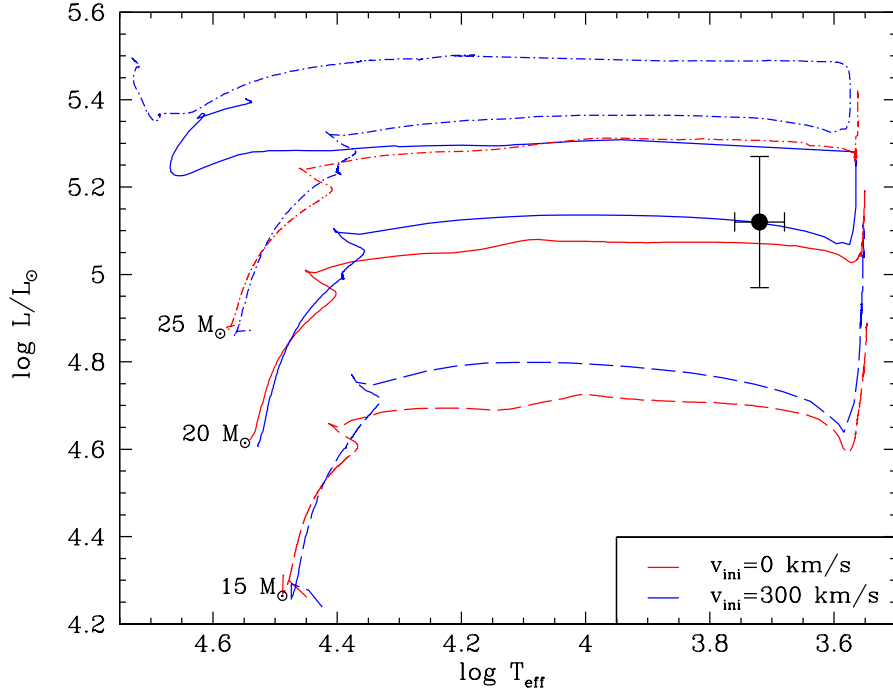


Fig. 3.— An HR diagram showing the L_{bol} and T_{eff} for the candidate progenitor of SN 2009kr (*filled circle*). Model stellar evolutionary tracks for solar metallicity (Hirschi et al. 2004) are also shown for a rotation of $v_{\text{ini}} = 0 \text{ km s}^{-1}$ (*dot-dashed, solid, and dashed red lines*) and $v_{\text{ini}} = 300 \text{ km s}^{-1}$ (*dot-dashed, solid, and dashed blue lines*).

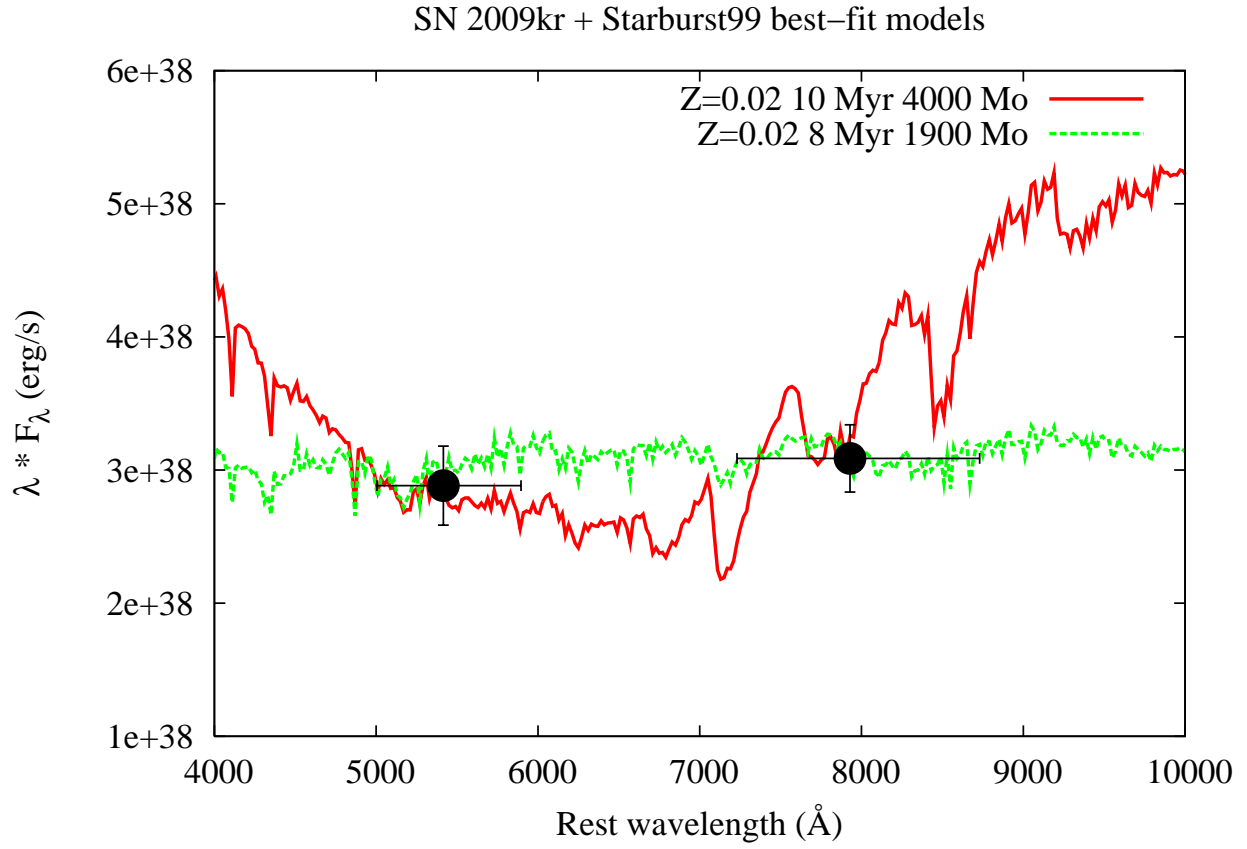


Fig. 4.— Comparison of the progenitor candidate (*filled circles*) with model spectral energy distributions for star clusters (Starburst99; Vazquez & Leitherer 2005; *lines*) for solar metallicity. The model parameters (age and total mass) are indicated in the legend.

Table 1. SN and Progenitor Candidate Position Comparison

	F555W (α/δ)	F814W (α/δ)
Uncertainty in the progenitor position (mas)	0/2	0/24
Uncertainty in the SN position (mas)	8/13	8/13
Geometric transformation (mas)	4/15	5/13
Total uncertainty (mas)	9/20	9/30
Difference in position (mas)	13/4	7/22

Note. — Uncertainties (1σ) in the SN and progenitor candidate right ascension (α) and declination (δ) positions for each band, in milliarcsec (mas), were estimated as the standard deviation of the average measurements. Uncertainties in the geometric transformation were derived from the differences in the fiducial star positions before and after the transformation. The total uncertainty is the quadrature sum of all uncertainties. The last row lists the residual difference between the SN and progenitor position after the geometric transformation. See text.